© 2017. Published by The Company of Biologists Ltd | Journal of Cell Science (2017) 130, 2359-2370 doi:10.1242/jcs.204537

RESEARCH ARTICLE

Control of mitochondrial homeostasis by endocytic regulatory proteins

Trey Farmer[1,2], James B. Reinecke[1,2], Shuwei Xie[1,2], Kriti Bahl[1,2], Naava Naslavsky[1,2,*] and Steve Caplan[1,2,*]

ABSTRACT

Mitochondria play essential roles in cellular energy processes, including ATP production, control of reactive oxygen species (ROS) and apoptosis. While mitochondrial function is regulated by the dynamics of fusion and fission, mitochondrial homeostasis remains incompletely understood. Recent studies implicate dynamin-2 and dynamin-related protein-1 (Drp1, also known as DNM1L), as GTPases involved in mitochondrial fission. Here, we identify the ATPase and endocytic protein EHD1 as a novel regulator of mitochondrial fission. EHD1 depletion induces a static and elongated network of mitochondria in the cell. However, unlike dynamin-2 and Drp1, whose depletion protects cells from staurosporine-induced mitochondrial fragmentation, EHD1-depleted cells remain sensitive to staurosporine, suggesting a different mechanism for EHD1 function. Recent studies have demonstrated that VPS35 and the retromer complex influence mitochondrial homeostasis either by Mul1-mediated ubiquitylation and degradation of the fusion protein Mfn2, or by removal of inactive Drp1 from the mitochondrial membrane. We demonstrate that EHD1 and its interaction partner rabankyrin-5 interact with the retromer complex to influence mitochondrial dynamics, likely by inducing VPS35-mediated removal of inactive Drp1 from mitochondrial membranes. Our study sheds light on mitochondrial dynamics, expanding a new paradigm of endocytic protein regulation of mitochondrial homeostasis.

KEY WORDS: Mitochondria, Fission, Retromer, EHD1, Endocytic recycling, VPS35, Rabankyrin-5, Dynamics

INTRODUCTION

Mitochondria play an essential role in cellular ATP production via oxidative phosphorylation, but are also crucial for regulating other cellular events including Ca^{2+} signaling (Duchen, 2000; Nicholls, 2005), apoptosis (Wang and Youle, 2009), reactive oxygen species (ROS) generation and sequestration (Hamanaka and Chandel, 2010), and others. Mitochondrial function is closely controlled by their dynamics, and they are continually undergoing cycles of fusion and fission, processes required for homeostasis and mitochondrial health (Chan, 2012). Indeed, perturbations of mitochondrial dynamics have been documented in a wide variety of neurodegenerative disorders, including Alzheimer's disease (Cho et al., 2009) and Parkinson's disease (PD) (Tang et al., 2015). Although the specific mechanisms by which mitochondrial dynamics influence many neurological disorders remain unclear, fusion and fission control mitochondrial size and shape, the number of mitochondria for inheritance in dividing cells, and many mitochondrial functions, such as respiration, cell survival, etc. (Chan, 2012; Flippo and Strack, 2017). Despite the high significance of the mitochondrial fusion and fission processes, and the identification of a growing number of molecules involved in these events, many questions remain unanswered regarding mechanisms of mitochondrial dynamics.

For mitochondrial fusion to occur, there need to be two distinct fusion events, between both the outer membranes and inner membranes of apposing mitochondria. To date, three mammalian GTPases have been implicated in mitochondrial fusion: the mitofusins Mfn1 and Mfn2 control fusion of the outer mitochondrial membrane (Rojo et al., 2002) (Santel and Fuller, 2001), and a protein mutated in dominant optic atrophy, OPA1, mediates fusion of the inner mitochondrial membrane (Alexander et al., 2000; Delettre et al., 2000). The dynamin-related GTPase Drp1 (also known as DNM1L), has been identified as a key protein required for mitochondrial fission (Bleazard et al., 1999; Labrousse et al., 1999). Drp1 is recruited from the cytosol by several mitochondrial membrane receptors, and functions in constriction and fission; its absence from the cell leads to an elongated and hyper-fused network of mitochondria (Frank et al., 2001). A recent study has also demonstrated that dynamin-2 (Dyn2, also known as DNM2) coordinates its fission activity with Drp1 to sequentially mediate the final step of mitochondrial division (Lee et al., 2016).

While identification of proteins involved directly in mitochondrial fusion and fission, and determining their mechanisms of action, has expanded rapidly in recent years, less is known about the regulation of mitochondrial dynamics. One exciting new area of research relates to recent studies pointing to a novel role for endocytic regulatory proteins in controlling mitochondrial dynamics. For example, VPS35, a member of the retromer cargo selection complex initially described for its role in recycling the mannose-6-phosphate receptor from endosomes back to the trans-Golgi network (Arighi et al., 2004), has been implicated as a key modulator of mitochondrial dynamics and one of only a handful of proteins that causes familial PD (Kumar et al., 2012; Vilarino-Guell et al., 2011; Zimprich et al., 2011). Indeed, the suppression of VPS35 expression in neonatal hippocampal neurons leads to a degenerative morphology with the generation of abnormal dendritic spines and swollen axons (Wang et al., 2012), and VPS35 expression is decreased in the substantia nigra of PD patients (MacLeod et al., 2013).

The mechanisms by which VPS35 and the retromer regulate mitochondrial dynamics and impact PD are not well understood. A recent study has demonstrated that VPS35 depletion in mouse dopamine neurons induces a PD-like condition, including neuronal death, α-synuclein deposition and fragmented mitochondria (Tang et al., 2015). VPS35 depletion or mutation also led to increased levels of the ubiquitin ligase Mul1, which ubiquitylates Mfn2 on the

[1]The Department of Biochemistry and Molecular Biology, The University of Nebraska Medical Center, Omaha, NE 68198, USA. [2]The Fred and Pamela Buffett Cancer Center, The University of Nebraska Medical Center, Omaha, NE 68198, USA.

*Authors for correspondence (scaplan@unmc.edu; nnaslavsky@unmc.edu)

S.C., 0000-0001-9445-4297

Received 24 March 2017; Accepted 31 May 2017

Journal of Cell Science (2017) 130, 2359-2370 doi:10.1242/jcs.204537

mitochondrial membrane, induces its proteasomal degradation, and may thus promote increased fission-to-fusion and fragmented mitochondria (Tang et al., 2015). Alternatively (or in parallel), a second study provides support for a different model for VPS35 function in the regulation of mitochondrial homeostasis and PD. Wang et al. demonstrate that VPS35 binds to complexes of inactive Drp1 on the mitochondrial membrane, and facilitates their removal and vesicular transport to lysosomes for degradation, thus freeing up new recruitment sites for active Drp1 and promoting fission and fragmentation (Wang et al., 2016, 2017).

In this study, we demonstrate that the endocytic fission protein and ATPase EHD1 is a novel player in mitochondrial dynamics. EHD1 depletion induces an elongated network of mitochondria that remain highly static over time. Despite having considerable similarity to the dynamin family of GTPases, unlike depletion of Drp1 or Dyn2, EHD1 knockdown did not prevent staurosporine (STS)-induced mitochondrial fragmentation, suggesting that it acts upstream of the mitochondrial fission proteins and more likely functions in a regulatory capacity. Indeed, as we have previously demonstrated that EHD1 and its binding partner rabankyrin-5 both interact with the retromer complex, we now hypothesize that EHD1 might regulate mitochondria through its control of VPS35. Our findings support a mechanism by which EHD1 and rabankyrin-5 interact with the retromer complex and influence mitochondrial dynamics by inducing VPS35-mediated removal of inactive Drp1 from the mitochondrial membrane.

RESULTS

EHD1 regulates mitochondrial fission

To address the potential role of EHD1 in mitochondrial fission and homeostasis, we depleted EHD1 from retinal pigment epithelial (RPE) cells by using siRNA. As demonstrated, siRNA-mediated knockdown of EHD1 was highly efficient with >90% of the protein depleted (Fig. 1E). To compare mitochondrial morphology in mock-treated and EHD1-depleted cells, we immunostained RPE cells with the mitochondrial membrane marker Tom20 (also known as TOMM20) (Fig. 1A–D). Compared to mock-treated cells, which display a typical network of mitochondria (Fig. 1A,C), cells lacking EHD1 displayed a very extended mitochondrial network, sporting numerous elongated structures (Fig. 1B,D). To quantitatively measure the differences in mitochondrial homeostasis between mock-treated and EHD1-depleted cells, we used the Mito Morphology Macro plug-in on ImageJ (http://imagejdocu.tudor.lu/doku.php?id=plugin:morphology:mitochondrial_morphology_macro_plug-in:start). Data from multiple cells imaged in three separate experiments indicate that both the average mitochondrial size (Fig. 1F) and average mitochondrial perimeter (Fig. 1G) are significantly larger in EHD1-depleted cells. On the other hand, the average circularity, which would be increased in a more fragmented mitochondrial network, is significantly decreased upon EHD1 depletion (Fig. 1H). To demonstrate the specificity of the EHD1 siRNA and rule out off-target effects, we ‘rescued’ the elongated mitochondrial phenotype observed upon EHD1 depletion by transfecting siRNA-resistant GFP–Myc–EHD1 into knockdown cells (Fig. S1). As demonstrated (Fig. S1A–F) and quantified (Fig. S1G), EHD1 knockdown cells transfected with reintroduced EHD1 displayed a mean mitochondrial length that was considerably shorter than that in knockdown cells, and was similar to that observed in mock-treated cells. Overall, these data support the notion that EHD1 plays a role in mitochondrial fission.

Based on the increased length of mitochondria upon EHD1 depletion, we hypothesized that if EHD1 mediates mitochondrial fission, then its absence should lead to more static and stabilized mitochondria compared with what would be seen in mock-treated cells. To test this, we used the mitochondria-specific dye Mitotracker Red to follow mitochondria in living cells. As demonstrated, in mock-treated cells, mitochondria are highly dynamic and are continually undergoing fusion and fission (Fig. 2A, see inset; Movie 1). The images were obtained every 15 s over 5 min, and the arrows highlight several events in which mitochondria undergo fission (Fig. 2A, see inset). In contrast, the elongated mitochondria in EHD1-depleted cells are very static, and limited dynamic movement can be observed over time (Fig. 2B; Movie 2). These experiments further support the notion that EHD1 is required for normal mitochondrial fission.

EHD1 likely functions upstream of the known mitochondrial fission proteins Dyn2 and Drp1

To date, the dynamin-related protein Drp1 is considered to be the major protein involved in mitochondrial fission (Pitts et al., 1999; Santel and Frank, 2008; Taguchi et al., 2007). However, a recent study has determined that the GTPase Dyn2 is also required for mitochondrial fission (Lee et al., 2016). Given the homology between EHD1 and dynamin (Daumke et al., 2007), and the role of EHD1 as an ATPase involved in endosomal fission (Cai et al., 2013, 2014; Jakobsson et al., 2011), we sought to explore the possibility that EHD1 may also act directly in mediating mitochondrial fission. To do so, we took advantage of a clever assay used by Lee et al. to identify the role of Dyn2 in mitochondrial fission (Lee et al., 2016). The broad-spectrum kinase inhibitor STS induces mitochondrial fission and fragmentation, but such fragmentation is prevented in cells lacking either Drp1 or Dyn2, highlighting their role in direct mitochondrial fission (Lee et al., 2016). We therefore rationalized that if EHD1 has a similar role, acting directly in mitochondrial fission, then EHD1 depletion should also prevent STS-induced mitochondrial fragmentation. Accordingly, mock- and EHD1-depleted cells were either treated or not with STS for 1 h, and then immunostained with antibodies to Tom20 to visualize mitochondria. Compared to mock-treated cells, EHD1-depleted cells displayed a network of elongated mitochondria (compare Fig. 3C to 3A). These mitochondria were larger in size (Fig. 3E) and had a greater average perimeter (Fig. 3F), but showed decreased circularity (Fig. 3G), consistent with our findings in Fig. 1. As anticipated, when mock-treated cells were stimulated with STS, this induced fission and fragmentation of mitochondria (compare Fig. 3B with 3A), and the STS-induced cells had mitochondria that were significantly smaller (Fig. 3E,F) with greater circularity (Fig. 3G). We then subjected EHD1-depleted cells to STS treatment. As demonstrated, fission and fragmentation of mitochondria were clearly observed (Fig. 3D), and the mitochondrial size, perimeter and circularity were not significantly different from the values we measured for mock cells induced with STS (Fig. 3E–G). While we cannot entirely rule out the possibility that EHD1 might act directly in mitochondrial fission, these data are generally consistent with the idea that unlike Drp1 and Dyn2, EHD1 does not act directly in mitochondrial fission, and may function upstream in a regulatory capacity.

EHD1 and rabankyrin-5 regulate retromer control of mitochondrial fission

Recent studies have identified an important role for the retromer cargo selection complex protein VPS35 in the regulation of mitochondrial homeostasis and PD (Kumar et al., 2012; Struhal et al., 2014; Vilarino-Guell et al., 2011; Wang et al., 2016a,b; Zimprich et al., 2011). One recently published mechanism suggests

Journal of Cell Science (2017) 130, 2359-2370 doi:10.1242/jcs.204537

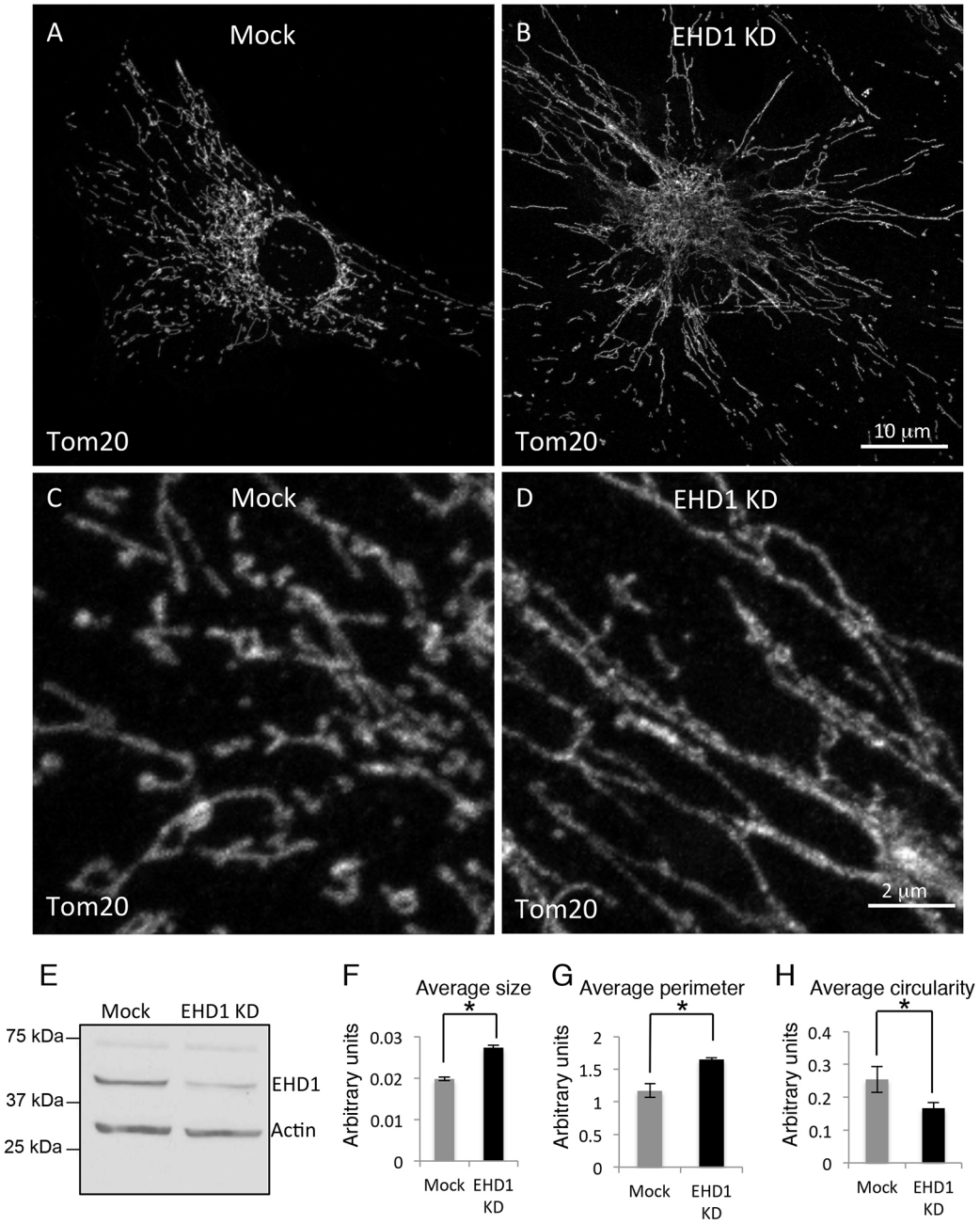

Fig. 1. EHD1 is required for mitochondrial homeostasis. (A–D) RPE cells were either mock treated (A,C) or treated with EHD1 siRNA for 72 h (B,D) and immunostained for the mitochondrial membrane marker Tom20. C and D are images of higher magnitude to visualize mitochondrial elongation. (E) The efficacy of the EHD1-depletion for A–D is demonstrated by immunoblotting lysates from mock and EHD1-depleted RPE cells. (F–H) The Mito Morphology Macro plugin in ImageJ was used to quantify mean±s.d. for mitochondrial size, perimeter and circularity, in three independent experiments each using 10 cells per treatment. **P*<0.05 (one-tailed Student's *t*-test).

that VPS35 controls the transport of the ubiquitin ligase Mul1 to the mitochondrial membrane (Tang et al., 2015). Mul1 then ubiquitylates the mitochondrial fusion protein Mfn2, inducing its proteasomal degradation (see model, Fig. 4A). Since we have previously demonstrated that both EHD1 and its binding partner rabankyrin-5 interact with the retromer complex, we hypothesized that EHD1 depletion might interfere with Mul1 relocation to the mitochondrial membrane, thus skewing the fission-to-fusion ratio toward fusion and elongated mitochondrial networks.

To test this idea, initially we set out to determine whether EHD1 interacts with Mul1. As a positive control, we confirmed that purified GST–EHD1 and the EH domain of EHD1 (EH1) pulled down the EHD1 interaction partner MICAL-L1 from bovine brain cytosol (Fig. 4B, top panel), consistent with our previous studies (Sharma et al., 2009). Likewise, the purified full-length GST–EHD1 pulled down Mul1 from the cytosol, whereas GST only and GST–EH1 did not (Fig. 4B, middle panel). To further address the relationship between EHD1, rabankyrin-5, the retromer and Mul1, we performed co-immunoprecipitation studies with lysates containing endogenous proteins (Fig. 4C). In these experiments, as anticipated, Mul1 clearly co-precipitated retromer components such as VPS26. However, in the same co-immunoprecipitations, we also

Journal of Cell Science (2017) 130, 2359-2370 doi:10.1242/jcs.204537

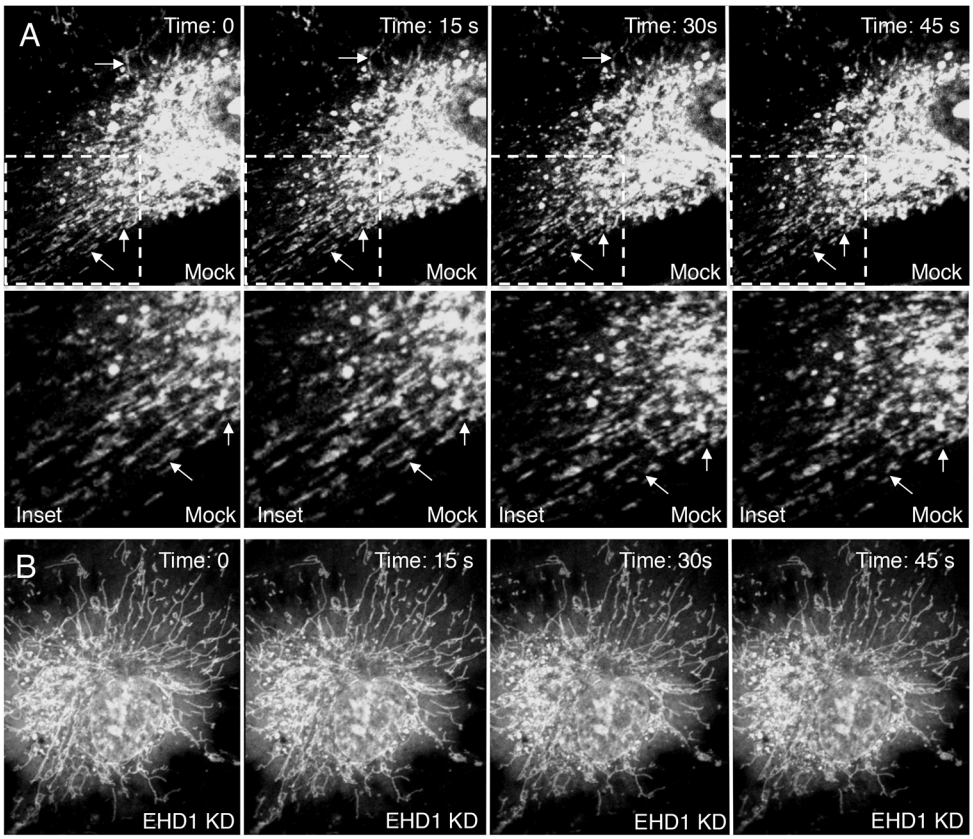

Fig. 2. Mitochondrial dynamics are impaired upon EHD1 depletion. Live imaging was performed on RPE cells incubated with Mitotracker Red and either mock treated (A) or treated with EHD1 siRNA for 72 h (B). 4-slice *z*-section images were taken every 15 s for 5 min for each treatment, and compiled to a maximal projection image. The arrows depict examples of fission events in mock-treated cells.

clearly detected the EHD1 interaction partner rabankyrin-5 (Fig. 4C), and low levels of EHD1 (data not shown). These data suggest that EHD1 and rabankyrin-5 may interact with Mul1 to mediate its transport to mitochondria, where it induces Mfn2 proteasomal degradation.

We rationalized that if rabankyrin-5 cooperates with EHD1 in the regulation of Mul1 transport to mitochondria, then depletion of rabankyrin-5 should result in a similar extended mitochondrial network to that seen upon EHD1 depletion. To test this idea, we used siRNA to knockdown rabankyrin-5 in RPE cells and immunostained them for Tom20. As demonstrated, compared to mock treatment, cells lacking rabankyrin-5 displayed an elongated mitochondrial network (compare Fig. 5B to 5A). Quantification of data from three separate experiments showed that the average size and perimeter of rabankyrin-5-depleted mitochondria were significantly greater than in mock-treated cells, whereas the average circularity significantly decreased in the knockdown cells (Fig. 5C).

Given that rabankyrin-5 is an EHD1 interaction partner (Zhang et al., 2012), we hypothesized that, similar to what is seen for EHD1, rabankyrin-5 may function upstream of Drp1 and Dyn2 in mitochondrial fission. To test this idea, we again used the STS assay (Lee et al., 2016) described in Fig. 3. As demonstrated in Fig. S2, rabankyrin-5 knockdown cells displayed elongated and extended mitochondria compared to mock-treated cells (compare Fig. S2C to S2A). Moreover, incubation of both mock-treated cells and rabankyrin-5 knockdown cells with STS led to mitochondrial fission as shown (compare Fig. S2B and S2D) and as quantified (Fig. S2E–G). These data are consistent with a role for rabankyrin-5 in the regulation of mitochondrial fission and homeostasis that is likely upstream of the fission proteins Drp1 and Dyn2.

Since the interaction between EHD1 and Mul1 was not as robust in immunoprecipitations as that observed between rabankyrin-5 and Mul1, and EHD1 interacts with rabankyrin-5 (Zhang et al., 2012), we hypothesized that perhaps rabankyrin-5 mediates the interaction between Mul1 and EHD1. To test this notion, we used lysate from mock-treated cells or cells treated with rabankyrin-5 siRNA in pulldown experiments with GST–EHD1. Using lysate from mock-treated cells, we observed significant Mul1 pulldown upon incubation with GST–EHD1, but not GST alone (Fig. 5D, top panel). However, upon efficient rabankyrin-5 depletion from the lysate (Fig. 5D, middle panel), very little Mul1 was pulled down by GST–EHD1 (Fig. 5D, top panel). These data suggest that EHD1 interacts with Mul1 via rabankyrin-5.

If EHD1 and rabankyrin-5 depletion promote elongated mitochondria by stabilizing the fusion protein Mfn2 on the mitochondrial membrane, one would predict that the knockdown of these proteins would result in accumulation of Mfn2. To test this hypothesis, we knocked down EHD1, rabankyrin-5 and VPS35, and compared the expression levels of Mfn2, as well as Drp1 and actin (control) in mock and depleted cells (Fig. 6A and quantified in B, D and F). siRNA-mediated knockdown resulted in efficient reduction in expression levels of all three proteins (Fig. 6A, top panels, and quantified in Fig. 6B–G), whereas actin levels remained very similar in mock- and siRNA-treated cells (Fig. 6A, bottom panels). However, no difference was observed in Mfn2 or Drp1 levels, and no major observable change in Drp1 association and/or distribution along mitochondrial membranes was noted [Fig. S3; compare A–C (mock) to D–F (EHD1 siRNA)]. These data suggest that despite the interaction between EHD1 and Mul1, preservation/accumulation of Mfn2 and/or Drp1 on the mitochondrial membrane did not appear to be the mechanism by which EHD1 depletion induced elongated mitochondrial networks.

Journal of Cell Science (2017) 130, 2359-2370 doi:10.1242/jcs.204537

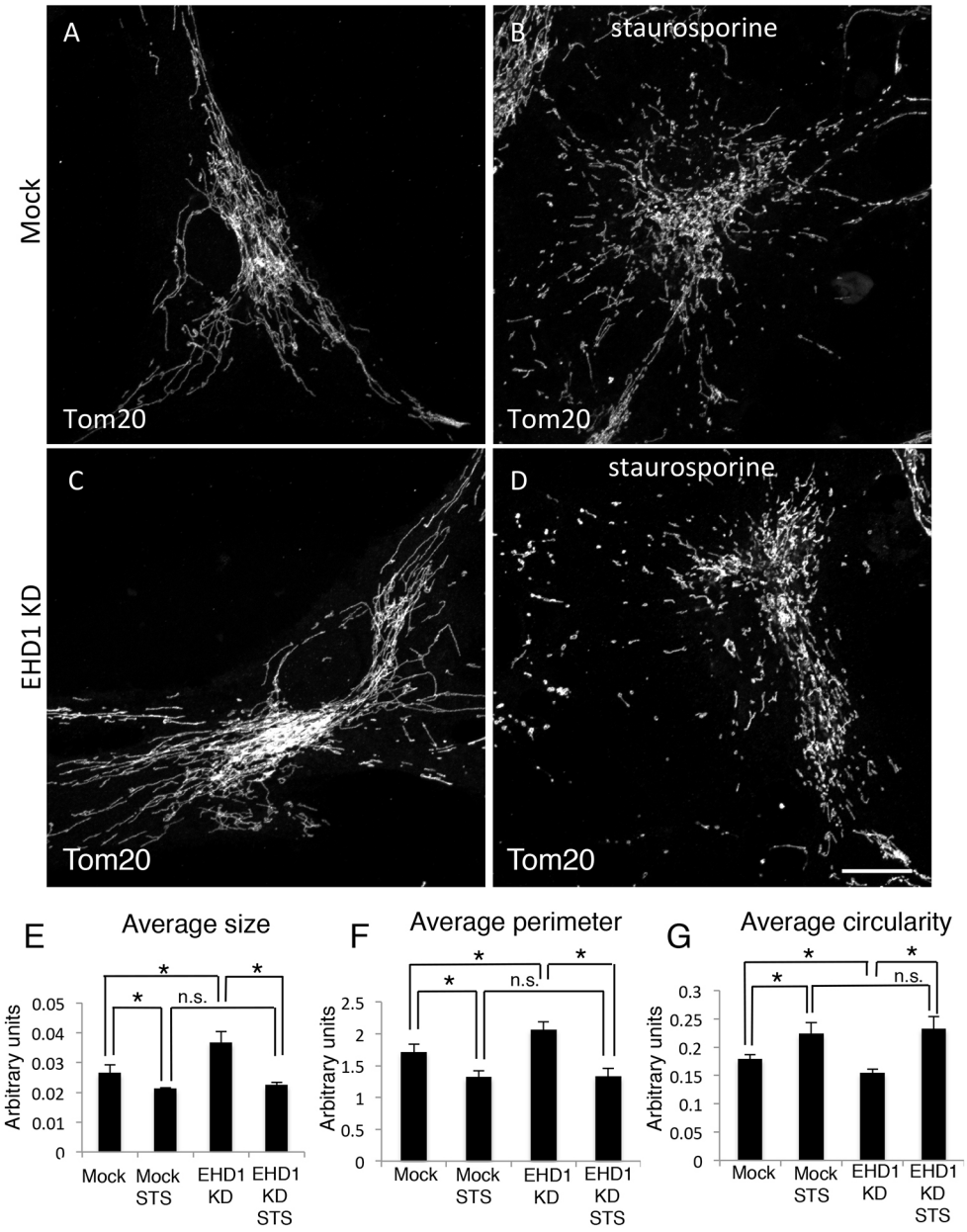

Fig. 3. EHD1 plays a regulatory role in mitochondrial fission. (A–D) RPE cells were either mock treated (A,B) or treated with EHD1 siRNA for 72 h (C,D), followed by incubation with STS for the last 1 h of treatment (B,D) or without the drug (A,C). (E–G) The Mito Morphology Macro plugin in ImageJ was used for quantifying mean ±s.d. for mitochondrial size, perimeter and circularity in three independent experiments each using 10 cells per treatment. *P<0.05; n.s., not statistically significant (one-tailed Student's t-test).

EHD1 and rabankyrin-5 differentially regulate VPS35 to control mitochondrial homeostasis

A recent study presents a new model by which VPS35 and the retromer may affect mitochondrial homeostasis; the model holds that VPS35 interacts with Drp1, and that vesicles containing VPS35 thus remove inactive Drp1 from the mitochondrial membrane, enabling active Drp1 to mediate fission (Wang et al., 2016b, and see Fig. 7L). By this scenario, depletion or sequestration of VPS35 would impair fission and induce hyper-elongation of mitochondria. We therefore hypothesized that EHD1, through its interaction with the retromer, might regulate the level of VPS35. To test this hypothesis, we immunoblotted lysates from cells that were either mock treated or treated with EHD1 siRNA (Fig. 7A). As demonstrated, under conditions where EHD1 was efficiently depleted, there was a consistent ∼50% decrease in the expression of VPS35, suggesting that the interaction between retromer and EHD1 stabilizes VPS35 levels (Fig. 7A, asterisk, and quantified in Fig. 7B). Indeed, the expression of an additional retromer cargo selection component, Vps26, was similarly decreased upon EHD1 knockdown (Fig. S4A,B). Moreover, these data support the model proposing that VPS35 and the retromer control mitochondrial fission by removing inactive Drp1 from the membrane, thereby allowing fission by available and active Drp1 (Fig. 7L).

We then tested whether rabankyrin-5, which both interacts with the retromer and influences mitochondrial dynamics, similarly affects VPS35 protein levels. Surprisingly, efficient siRNA-mediated depletion of rabankyrin-5 had no effect on VPS35 expression (Fig. 7C, quantified in 7D), leading us to hypothesize that rabankyrin-5 mechanistically regulates VPS35 function in a manner distinct from that of EHD1. One possibility was that rabankyrin-5 is needed for the trafficking of VPS35 from endosomes to the mitochondrial membrane. We therefore argued that if rabankyrin-5 is required for this transport step, then its depletion should lead to an altered VPS35 localization pattern within the cell. To test this, we knocked down rabankyrin-5, and compared the subcellular distribution of VPS35 to that observed in mock-treated cells, using GM130 (also known as

Journal of Cell Science (2017) 130, 2359-2370 doi:10.1242/jcs.204537

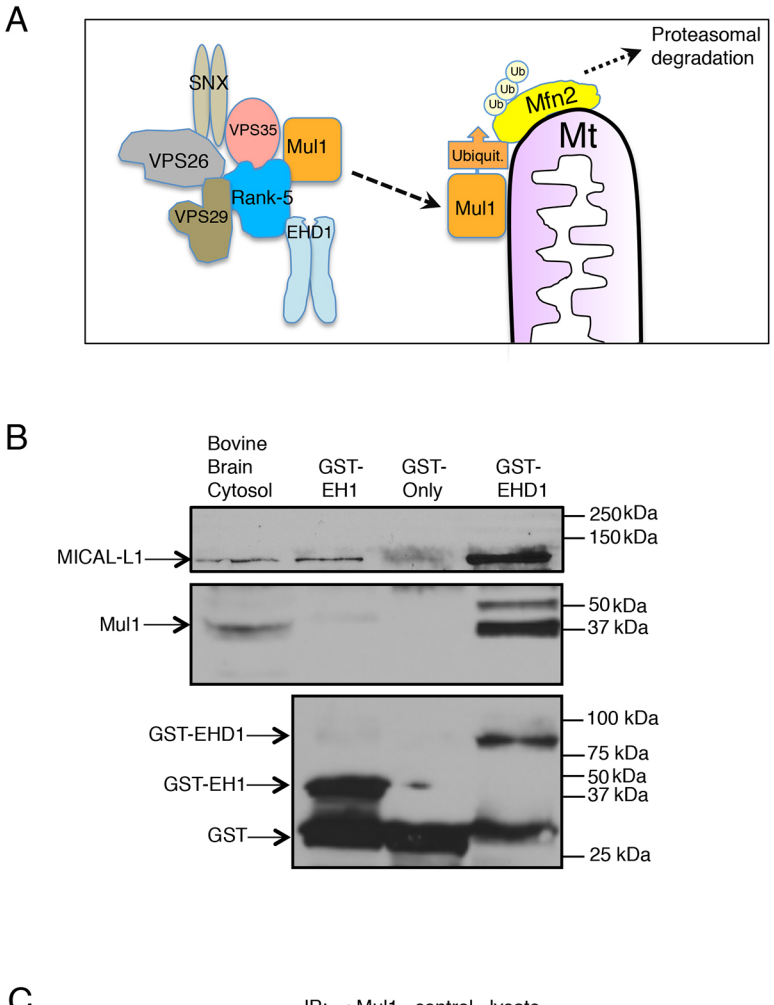

Fig. 4. EHD1 interacts with Mul1. (A) Model for the potential role of EHD1 in regulating mitochondrial dynamics via Mul1. Under normal conditions, the ubiquitin ligase Mul1 is released from an interaction with VPS35 and the retromer components (including EHD1), and relocates to the mitochondrial membrane, where it ubiquitylates Mfn2, inducing its proteasomal degradation and promoting normal mitochondrial fission. Upon EHD1 depletion, Mul1 would be retained in association with VPS35 and the retromer, preventing Mfn2 degradation and thus enhancing mitochondrial membrane fusion. (B) GST pulldown from bovine brain cytosol was performed with GST only, a GST-tagged EH domain of EHD1 (GST–EH1) and GST–EHD1. Eluates were immunoblotted with antibodies against MICAL-L1 (top panel), as a positive interactor with EHD1, and Mul1 (middle panel). GST fusion protein samples were immunoblotted with anti-GST (bottom panel). (C) Co-immunoprecipitation (IP) of proteins from a HeLa cell lysate using anti-Mul1 (αMul1), and immunoblotted with anti-Vps26 and anti-rabankyrin-5 antibodies. 25 kDa immunoglobulin light chains detected by the secondary anti-light chain antibody are indicated in the bottom panel.

GOLGA2) to mark the Golgi region as a reference point within the cell (Fig. 7E–J). As demonstrated, compared to VPS35 distribution in mock-treated cells, upon rabankyrin-5-depletion there was a significant degree of sequestration of VPS35 in the Golgi region of the cell (Fig. 7, compare F and H to E and G; dashed regions of interest are the Golgi, as marked by GM130 in I and J). To quantify the difference observed, we measured the VPS35 fluorescence localized to the Golgi region in knockdown cells and found that it was significantly increased compared to mock-treated cells (Fig. 7K). Overall, these data support a model by which depletion of EHD1 and rabankyrin-5 lead to reduced VPS35 levels or an altered VPS35 subcellular distribution, respectively. This in turn may prevent removal of inactive Drp1 from mitochondrial membranes, culminating in impaired fission, thus leading to the hyper-elongated mitochondrial network observed in these cells (Fig. 7L).

DISCUSSION

Mitochondrial dynamics have long been correlated with their physiological functions, and their structures appear along a continuum from tubular networks to smaller fragmented membranes (Benard et al., 2006). Indeed, early observations found that, upon activation of ATP synthesis, mitochondria displayed a smaller and more-condensed phenotype (Hackenbrock, 1966). Mitochondrial fragmentation has also been observed in patient fibroblasts that have altered energy production due to defects in respiratory chain subunits (Capaldi et al., 2004; Koopman et al., 2005). Since mitochondrial dynamics are controlled by a tight balance between fusion and fission, much attention has been placed on identifying the proteins involved in these processes. In particular, until recently, the role of fission was thought to be mediated primarily by a single dynamin-related protein, Drp1 (Bleazard et al., 1999; Labrousse et al., 1999). However, a recent study sheds new light on the fission process and has identified Dyn2 as playing a sequential role with Drp1 in the cleavage of mitochondrial membranes (Lee et al., 2016).

In addition to focus on the proteins carrying out the process of fission, recent works have also highlighted rapid developments in our understanding of the regulation of Drp1- and Dyn2-mediated

Journal of Cell Science (2017) 130, 2359-2370 doi:10.1242/jcs.204537

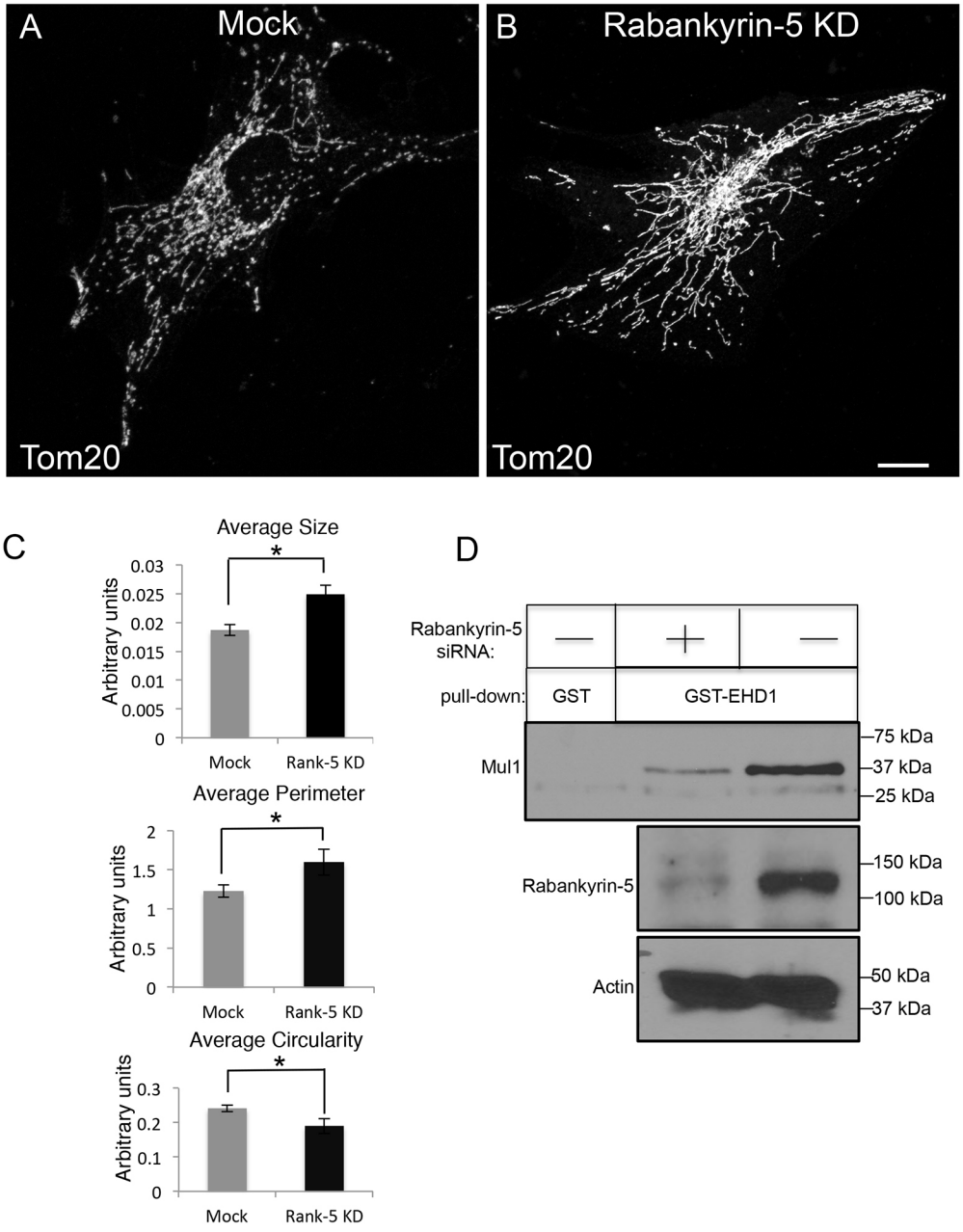

Fig. 5. Rabankyrin-5 mediates the interaction between EHD1 and Mul1, and its depletion induces an elongated mitochondrial network similar to that observed upon EHD1 depletion. (A,B) RPE cells were either mock treated (A) or treated with rabankyrin-5 siRNA for 72 h (B) and immunostained for the mitochondrial membrane marker Tom20. (C) The Mito Morphology Macro plugin in ImageJ was used for quantifying mean±s.d. for mitochondrial size, perimeter and circularity in three independent experiments each using 10 cells per treatment. **P*<0.05 (one-tailed Student's *t*-test). (D) HeLa cells were either mock treated or treated with rabankyrin-5 siRNA, lysed, and subjected to a GST–EHD1 pulldown, and immunoblotted with Mul1 (upper panel). The efficacy of the rabankyrin-5-depletion is demonstrated by immunoblotting lysates from mock-treated and rabankyrin-5-depleted cells (bottom two panels).

mitochondrial fission. Exciting new studies implicate the VPS35 retromer subunit and the retromer complex in PD and mitochondrial fission, forging a novel connection between an endocytic regulatory complex and a non-endocytic organelle (Follett et al., 2014; Kumar et al., 2012; Sharma et al., 2012; Struhal et al., 2014; Tang et al., 2015; Vilarino-Guell et al., 2011; Zimprich et al., 2011). However, while the relationship between VPS35, mitochondrial dynamics and PD is now irrefutable, the precise mechanism(s) by which VPS35 influences mitochondrial morphology remain somewhat controversial.

In our study, we identify a novel regulatory role for EHD1 as a potent effector of mitochondrial homeostasis. We demonstrated that EHD1 depletion leads to a highly static and elongated mitochondrial network reminiscent of that seen upon Drp1 depletion (Benard et al., 2006). Given that EHD1 is an ATPase that displays homology to the dynamin family (Daumke et al., 2007; Melo et al., 2017), this raised the possibility that it could play a role directly in fission, in a similar manner to that of Drp1 and Dyn2. However, the failure to observe significant levels of EHD1 associated with the mitochondrial membrane reduced the likelihood of such a direct function. Additionally, whereas STS treatment failed to induce mitochondrial fragmentation in either Drp1- or Dyn2-depleted cells (Lee et al., 2016), STS did cause fragmentation in EHD1-depleted cells. This suggests that the kinase inhibitor likely acts directly on Drp1 and/or Dyn2, bypassing a potential regulatory role carried out by EHD1.

What could the potential role of EHD1 be in regulating mitochondrial fission upstream of Drp1/Dyn2? Studies by our group and others have linked EHD1 to the retromer complex (Gokool et al., 2007; Zhang et al., 2012), suggesting the intriguing possibility that EHD1 might somehow function upstream of the mitochondrial fission proteins. One potential mechanism by which VPS35 and the retromer have been proposed to regulate mitochondrial fission is via the ubiquitin ligase Mul1 (Tang et al.,

Journal of Cell Science (2017) 130, 2359-2370 doi:10.1242/jcs.204537

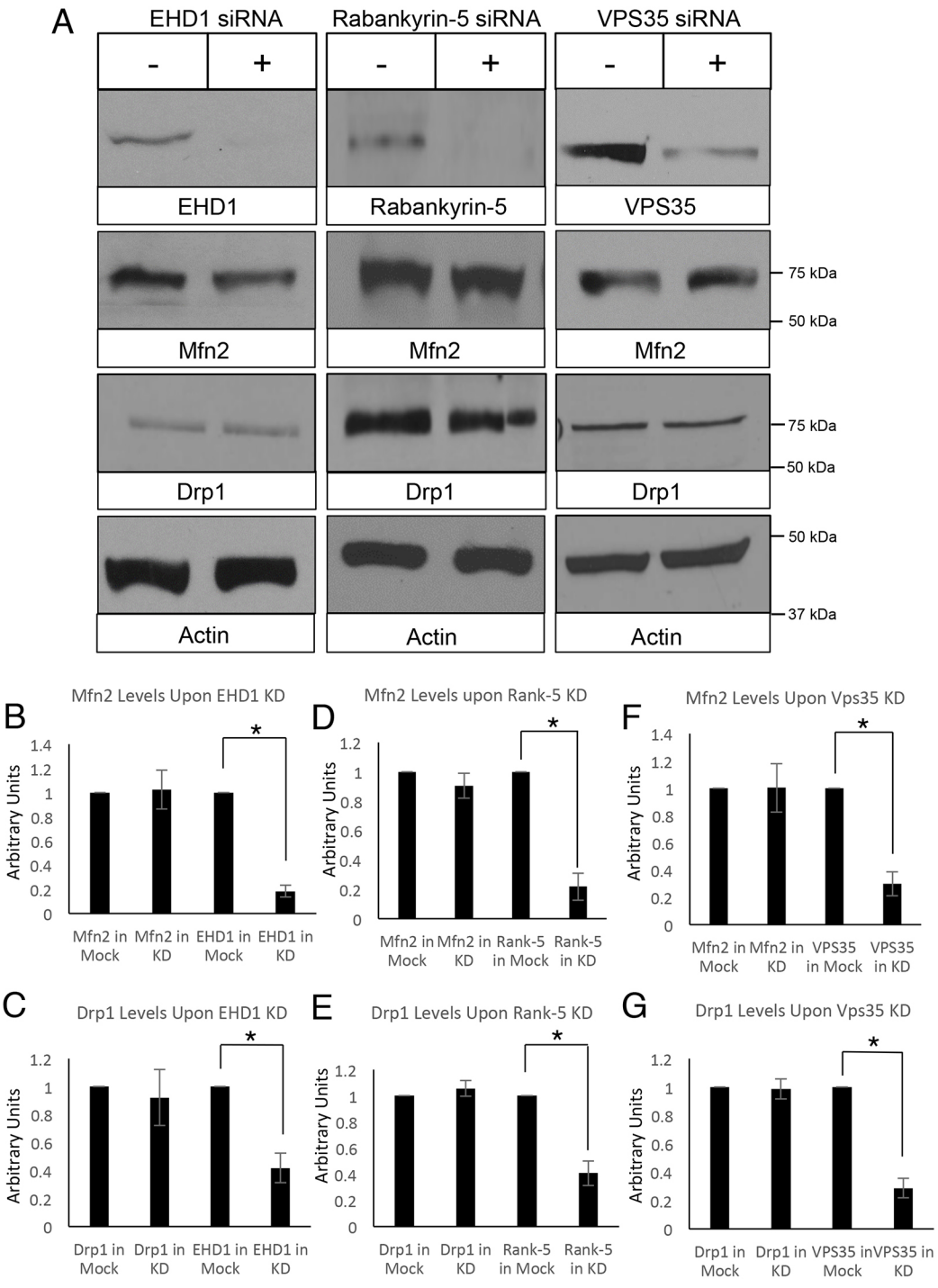

Fig. 6. Depletion of EHD1, rabankyrin-5 or VPS35 does not induce Mfn2 accumulation. HeLa cells were either mock treated, or treated with EHD1, rabankyrin-5 or Vps35 siRNA for 72 h. Depletion efficacy was validated by immunoblotting with antibodies against EHD1, rabankyrin-5 and VPS35 (A; top three panels), and the effect of the siRNA was assessed with antibodies against Mfn2 (A; second panel from the top), Drp1 (A; third panel from the top) and actin (A; bottom panel). (B–G) Densitometric quantification from three separate experiments. *P<0.05 (one-tailed Student's t-test).

2015; Yun et al., 2014). Mul1 interacts with VPS35, and, in this scenario, release of Mul1 from this interaction is thought to facilitate Mul1 transport to the mitochondrial membrane, where it ubiquitylates the fusion-promoting protein Mfn2, sending it for proteasomal degradation and thus inducing a more-fragmented mitochondrial phenotype (Tang et al., 2015). While we did demonstrate that Mul1 interacts with EHD1, through the EHD1 interaction partner rabankyrin-5, which also interacts with the retromer (Zhang et al., 2012), we did not find increased levels of Mfn2 as would be anticipated if less proteasomal degradation occurs. This suggests that EHD1/VPS35 regulation of Mul1 is not the primary mechanism for the control of mitochondrial dynamics.

It has also been proposed that VPS35 regulates mitochondrial dynamics by a different mechanism, whereby VPS35-containing vesicles interact with inactive Drp1 on the mitochondrial membrane, removing the inactive Drp1 fission-promoting protein.

Journal of Cell Science (2017) 130, 2359-2370 doi:10.1242/jcs.204537

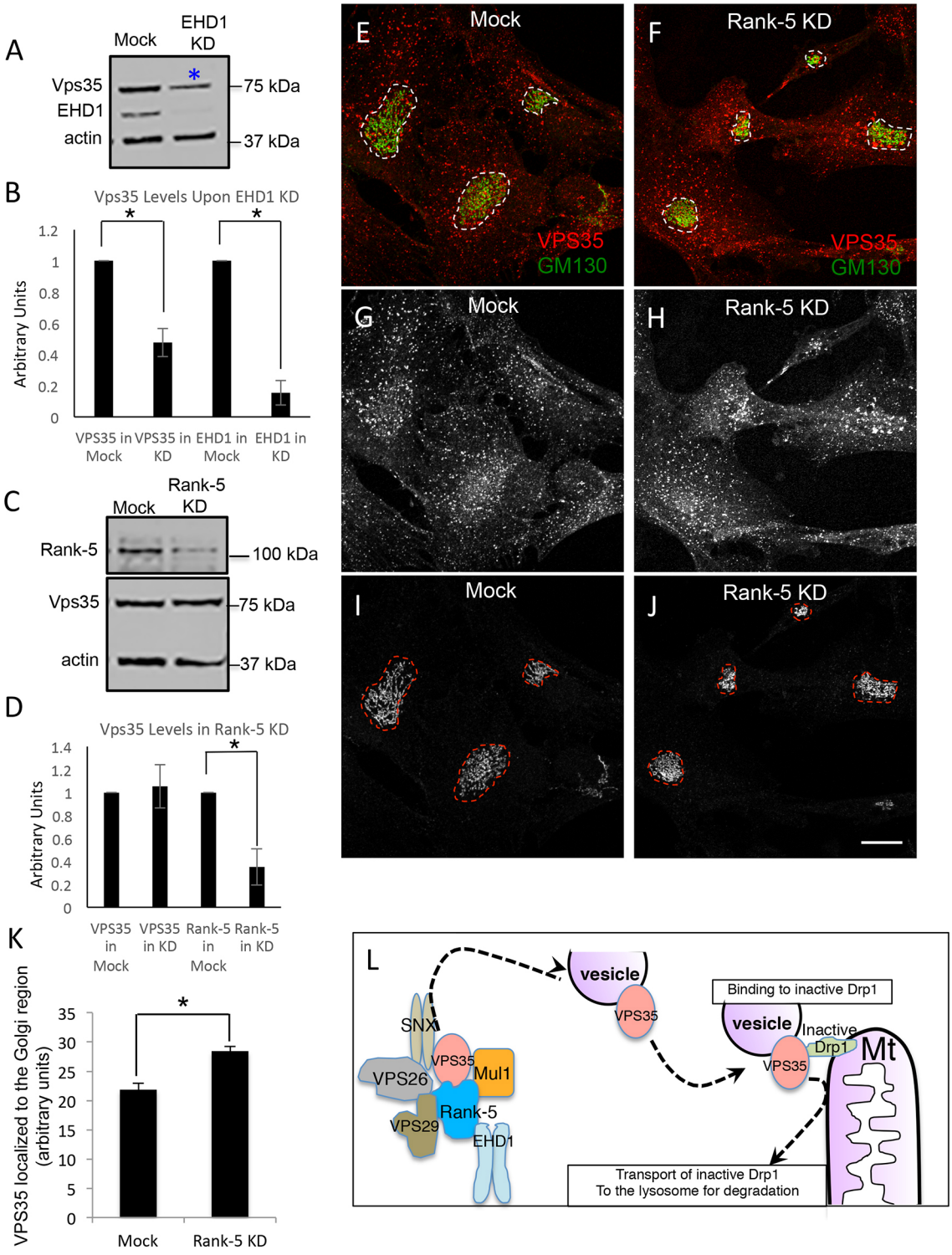

Fig. 7. Depletion of EHD1 and rabankyrin-5 results in reduced and sequestered VPS35, respectively. (A–D) HeLa cells were either mock treated, treated with EHD1 siRNA (A) or treated with rabankyrin-5 (Rank-5) siRNA (C) for 72 h and immunoblotted for VPS35, EHD1, Rank-5 and actin. The asterisk (in A) indicates reduced VPS35 protein levels. (B,D) Quantification of protein levels from three independent experiments. *P<0.05 (one-tailed Student's t-test). (E–J) RPE cells were either mock treated (E,G,I) or treated with rabankyrin-5 siRNA for 72 h (F,H,J), and immunostained for VPS35 and the Golgi membrane marker GM130. Regions of interest were drawn with a dashed line around the GM130 Golgi stain (I,J) and superimposed in the merged images (E,F) and in the VPS35-stained images (G,H; note, the region of interest is not shown in G and H so the VPS35 distribution pattern can be observed more clearly). Scale bar: 10 µm. (K) ImageJ was used to quantify the mean±s.d. for fluorescence of VPS35 localized to the central Golgi region marked by the regions of interest in three independent experiments each using 10 cells per treatment. *P<0.05 (one-tailed Student's t-test). (L) Current working model showing the proposed mechanism for EHD1 regulation of mitochondrial dynamics. In this scenario, EHD1 might act in facilitating fission of vesicles that transport VPS35 from endosomes to the mitochondrial membrane. VPS35 might then interact with inactive Drp1, removing it from the mitochondrial membrane and facilitating the function of active Drp1 leading to mitochondrial fission. Thus, the absence of EHD1 might prevent this transport step and lead to elongated mitochondria.

Journal of Cell Science

Journal of Cell Science (2017) 130, 2359-2370 doi:10.1242/jcs.204537

This is turn frees mitochondrial membrane space for new active Drp1, thus leading to fission (Wang et al., 2016b). Under this scenario, loss of VPS35, or potentially its altered regulation in the absence of EHD1, could lead to impaired fission, resulting in the generation of an elongated and static mitochondrial network. Indeed, we observed decreased VPS35 expression upon EHD1 depletion, providing support for this idea. Surprisingly, rabankyrin-5-depletion did not induce a similar decrease in VPS35 levels to that observed upon EHD1 depletion. However, rabankyrin-5 depletion did cause an altered subcellular distribution of VPS35, providing a mechanism, albeit different from that of EHD1, for the formation of elongated mitochondrial networks. While we cannot rule out other potential mechanisms for the involvement of EHD1 and rabankyrin-5 in the regulation of mitochondrial homeostasis, including the possibility that EHD1 might serve (at least in part) as a direct mitochondrial fission protein, to date our studies broadly support a more regulatory role for these proteins upstream of the mitochondrial membrane.

In summary, our study highlights a new layer of regulation of mitochondrial dynamics, and further tightens the growing crosstalk between endocytic and mitochondrial pathways. Although, to date, mutations or impaired expression levels of EHD1 and rabankyrin-5 have not been implicated in PD, the expansion of key mitochondrial regulatory proteins to additional retromer components (and their interaction partners) is likely to shed new light on mechanisms of PD.

MATERIALS AND METHODS

Reagents and antibodies

Mitotracker Red was purchased from Thermo Fisher Scientific. STS was purchased from Sigma-Aldrich. Antibodies against the following proteins were used: EHD1 (ab109311, 1:1000 dilution for immunoblotting), Vps26 (ab23892, 1:500 dilution for immunoblotting), VPS35 (ab97545, 1:500 dilution for immunoblotting), Mfn2 (ab56889, 1:500 dilution for immunoblotting) and actin (ab14128, 1:4000 dilution for immunoblotting) from Abcam; Tom20 (sc-11415, Santa Cruz Biotechnology, 1:1000 dilution for immunofluorescence); Mul1 (GTX112673, GeneTex, 1:500 dilution for immunoblotting); GST conjugated to horseradish peroxidase (HRP) (NA935, Amersham, 1:5000 dilution for immunoblotting); MICAL-L1 (H00085377-B01P, Abnova, 1:500 dilution for immunoblotting); rabankyrin-5 (PA5-24640, Thermo Scientific, 1:200 dilution for immunoblotting); Drp1 (8570s, Cell Signaling, 1:500 dilution for immunoblotting); GM130 (610822, BD Biosciences, 1:500 dilution for immunoblotting); donkey anti-mouse IgG light chain conjugated to HRP (715-035-151, 1:10,000 dilution for immunoblotting), mouse anti-rabbit IgG light chain conjugated to HRP (211-032-171, 1:10,000 dilution for immunoblotting), from Jackson; and donkey anti-mouse-IgG conjugated to Alexa Fluor 488 (A21202, 1:700 dilution for immunofluorescence), donkey anti-mouse-IgG conjugated to Alexa Fluor 568 (21043, 1:700 dilution for immunofluorescence), goat anti-rabbit-IgG Alexa Fluor 488 (A11034, 1:700 dilution for immunofluorescence), and goat anti-rabbit-IgG conjugated to Alexa Fluor 568 (A11036, 1:700 dilution for immunofluorescence) from Molecular Probes.

Cell culture

The HeLa cervical cancer cell line was obtained from the American Type Culture Collection (ATCC) and grown in DMEM (high glucose) containing 10% fetal bovine serum (FBS), 1× penicillin-streptomycin (Invitrogen) and 2 mM glutamine. The immortalized retinal pigment epithelium (RPE) cell line from the ATCC was grown in DMEM/F12 containing 10% FBS, 1× penicillin-streptomycin and 2 mM glutamine. Cell lines were routinely tested for mycoplasma contamination.

siRNA transfections and rescue experiments

Custom EHD1 siRNA oligonucleotide (Sharma et al., 2009), and On-Target rabankyrin-5 siRNA oligonucleotides were obtained from Dharmacon. RPE cells were transfected using Liptofectamine RNAiMAX (Invitrogen) with 40 nM oligonucleotide. The efficiency of protein knockdown was measured at 72 h post transfection by immunoblotting or immunofluorescence for each experiment. For rescue experiments, RPE cells were simultaneously treated for EHD1 siRNA and transfected using Fugene 6 (Roche) with a GFP–Myc–EHD1 construct engineered with silent mutations rendering it resistant to the siRNA oligonucleotides.

Immunoblotting

Cells were washed twice in ice-cold PBS and were then scraped off plates with a rubber policeman into ice-cold lysis buffer (50 mM Tris-HCl pH 7.4, 100 mM NaCl, 0.5% Triton X-100 and 1× protease cocktail inhibitor). Protein levels of postnuclear lysates were quantified by using the Bradford assay for equal protein level loading. For immunoblotting, 20–30 µg of protein per lysate (from either RPE or HeLa cells) were separated by 10% SDS-PAGE. Proteins were transferred onto nitrocellulose membranes, and blocked for 30 min at room temperature in PBS with 0.3% Tween 20 and 5% non-fat dry milk (PBST). The membranes were then incubated overnight with primary antibodies diluted in PBST. Membranes were washed with TBST and then incubated with the appropriate secondary antibody in PBST for 30 min.

Quantification of immunoblots

The adjusted relative density of the immunoblots was measured in ImageJ according to the following protocol: http://www1.med.umn.edu/starrlab_deleteme/prod/groups/med/@pub/@med/@starrlab/documents/content/med_content_370494.html.

Quantification of mitochondrial parameters

The average size, perimeter, and circularity of mitochondria were measured in ImageJ, using a plugin called Mito Morphology Macro (http://imagejdocu.tudor.lu/doku.php?id=plugin:morphology:mitochondrial_morphology_macro_plug-in:start). Images of Tom20-stained cells were imported into ImageJ where the program was able to set a common threshold and calculate the mitochondrial parameters.

Quantification of VPS35 subcellular distribution

The distribution of VPS35-containing vesicles was assessed in ImageJ. Multi-channel images were split into separate channels. An area was drawn around the Golgi region as marked by the Golgi marker GM130, using the 'free hand' tool. This region was then superimposed on the image of the VPS35 immunostaining, and the mean VPS35 fluorescence intensity of that region was measured and calculated.

Immunofluorescence

RPE cells were treated as indicated in the text and then fixed in 4% paraformaldehyde in PBS for 10 min at room temperature. Cells were rinsed three times in PBS. The cells were then incubated with primary antibody in PBS containing 0.5% BSA and 0.2% saponin for 1 h at room temperature, washed three times in PBS and then incubated with the appropriate fluorochrome-conjugated secondary antibodies diluted in PBS containing 0.5% BSA and 0.2% saponin for 30 min. Cells were washed three times in PBS and mounted in Fluoromount.

Using a Zeiss LSM800 confocal microscope with a 63×1.4 NA oil objective, *z*-stack confocal images were collected. The series of images from a *z*-stack was then processed to yield a maximal projection image using the Zeiss Zen software. For quantification, collected maximal projection images were imported into ImageJ as described above.

Live imaging

RPE cells were plated on 35 mm glass-bottom plates and transfected with the appropriate siRNA treatment. At 72 h post transfection, the cells were treated with 25 nM Mitotracker Red for 15 min in Opti-mem media. The cells were then washed two times with DMEM/F12 (no Phenol Red), and 10% FBS was added to the cells.

Using the system described above, a four slice *z*-stack image was taken every 15 s for 5 min. Each time-point *z*-stack was then converted into a

maximal projection image as described above. Image quantification was performed as described above.

STS assay

RPE cells were treated with 1 µM STS (Sigma Aldrich) for the last 1 h of a 72 h siRNA transfection. The cells then underwent processing for immunofluorescence as described above.

Statistics

Data from ImageJ was imported into Microsoft Excel. The mean and the s.d. were calculated from data obtained from three independent experiments with at least 10 images taken per treatment. Statistical significance was calculated using a Student's *t*-test with the Vassarstats program (http://www.vassarstats.net).

Acknowledgements

The authors wish to thank Dr H. Fox (UNMC) for very helpful discussions.

Competing interests

The authors declare no competing or financial interests.

Author contributions

Conceptualization: T.F., J.R., N.N., S.C.; Formal analysis: T.F.; Investigation: T.F., J.R., S.X., K.B., N.N.; Data curation: T.F.; Writing - original draft: T.F., S.C.; Writing - review & editing: J.R., N.N., S.C.; Supervision: N.N., S.C.; Project administration: S.C.; Funding acquisition: S.C.

Funding

We are grateful to grant support from the National Institutes of Health, National Institute of General Medical Sciences (grant R01GM074876), and an Institutional Development Award from the National Institutes of General Medical Sciences (P30GM106397). Deposited in PMC for release after 12 months.

Supplementary information

Supplementary information available online at
http://jcs.biologists.org/lookup/doi/10.1242/jcs.204537.supplemental

References

Alexander, C., Votruba, M., Pesch, U. E. A., Thiselton, D. L., Mayer, S., Moore, A., Rodriguez, M., Kellner, U., Leo-Kottler, B., Auburger, G. et al. (2000). OPA1, encoding a dynamin-related GTPase, is mutated in autosomal dominant optic atrophy linked to chromosome 3q28. *Nat. Genet.* **26**, 211-215.

Arighi, C. N., Hartnell, L. M., Aguilar, R. C., Haft, C. R. and Bonifacino, J. S. (2004). Role of the mammalian retromer in sorting of the cation-independent mannose 6-phosphate receptor. *J. Cell Biol.* **165**, 123-133.

Benard, G., Faustin, B., Passerieux, E., Galinier, A., Rocher, C., Bellance, N., Delage, J.-P., Casteilla, L., Letellier, T. and Rossignol, R. (2006). Physiological diversity of mitochondrial oxidative phosphorylation. *Am. J. Physiol. Cell Physiol.* **291**, C1172-C1182.

Bleazard, W., McCaffery, J. M., King, E. J., Bale, S., Mozdy, A., Tieu, Q., Nunnari, J. and Shaw, J. M. (1999). The dynamin-related GTPase Dnm1 regulates mitochondrial fission in yeast. *Nat. Cell Biol.* **1**, 298-304.

Cai, B., Giridharan, S. S. P., Zhang, J., Saxena, S., Bahl, K., Schmidt, J. A., Sorgen, P. L., Guo, W., Naslavsky, N. and Caplan, S. (2013). Differential roles of C-terminal Eps15 homology domain proteins as vesiculators and tubulators of recycling endosomes. *J. Biol. Chem.* **288**, 30172-30180.

Cai, B., Xie, S., Caplan, S. and Naslavsky, N. (2014). GRAF1 forms a complex with MICAL-L1 and EHD1 to cooperate in tubular recycling endosome vesiculation. *Front Cell Dev. Biol.* **2**, 22.

Capaldi, R. A., Murray, J., Byrne, L., Janes, M. S. and Marusich, M. F. (2004). Immunological approaches to the characterization and diagnosis of mitochondrial disease. *Mitochondrion* **4**, 417-426.

Chan, D. C. (2012). Fusion and fission: interlinked processes critical for mitochondrial health. *Annu. Rev. Genet.* **46**, 265-287.

Cho, D.-H., Nakamura, T., Fang, J., Cieplak, P., Godzik, A., Gu, Z. and Lipton, S. A. (2009). S-nitrosylation of Drp1 mediates beta-amyloid-related mitochondrial fission and neuronal injury. *Science* **324**, 102-105.

Daumke, O., Lundmark, R., Vallis, Y., Martens, S., Butler, P. J. G. and McMahon, H. T. (2007). Architectural and mechanistic insights into an EHD ATPase involved in membrane remodelling. *Nature* **449**, 923-927.

Delettre, C., Lenaers, G., Griffoin, J.-M., Gigarel, N., Lorenzo, C., Belenguer, P., Pelloquin, L., Grosgeorge, J., Turc-Carel, C., Perret, E. et al. (2000). Nuclear gene OPA1, encoding a mitochondrial dynamin-related protein, is mutated in dominant optic atrophy. *Nat. Genet.* **26**, 207-210.

Duchen, M. R. (2000). Mitochondria and calcium: from cell signalling to cell death. *J Physiol* **529**, 57-68.

Flippo, K. H. and Strack, S. (2017). Mitochondrial dynamics in neuronal injury, development and plasticity. *J. Cell Sci.* **130**, 671-681.

Follett, J., Norwood, S. J., Hamilton, N. A., Mohan, M., Kovtun, O., Tay, S., Zhe, Y., Wood, S. A., Mellick, G. D., Silburn, P. A. et al. (2014). The Vps35 D620N mutation linked to Parkinson's disease disrupts the cargo sorting function of retromer. *Traffic* **15**, 230-244.

Frank, S., Gaume, B., Bergmann-Leitner, E. S., Leitner, W. W., Robert, E. G., Catez, F., Smith, C. L. and Youle, R. J. (2001). The role of dynamin-related protein 1, a mediator of mitochondrial fission, in apoptosis. *Dev. Cell* **1**, 515-525.

Gokool, S., Tattersall, D. and Seaman, M. N. J. (2007). EHD1 interacts with retromer to stabilize SNX1 tubules and facilitate endosome-to-Golgi retrieval. *Traffic* **8**, 1873-1886.

Hackenbrock, C. R. (1966). Ultrastructural bases for metabolically linked mechanical activity in mitochondria. I. Reversible ultrastructural changes with change in metabolic steady state in isolated liver mitochondria. *J. Cell Biol.* **30**, 269-297.

Hamanaka, R. B. and Chandel, N. S. (2010). Mitochondrial reactive oxygen species regulate cellular signaling and dictate biological outcomes. *Trends Biochem. Sci.* **35**, 505-513.

Jakobsson, J., Ackermann, F., Andersson, F., Larhammar, D., Low, P. and Brodin, L. (2011). Regulation of synaptic vesicle budding and dynamin function by an EHD ATPase. *J. Neurosci.* **31**, 13972-13980.

Koopman, W. J. H., Visch, H.-J., Verkaart, S., van den Heuvel, L. W. P. J., Smeitink, J. A. M. and Willems, P. H. G. M. (2005). Mitochondrial network complexity and pathological decrease in complex I activity are tightly correlated in isolated human complex I deficiency. *Am. J. Physiol. Cell Physiol.* **289**, C881-C890.

Kumar, K. R., Weissbach, A., Heldmann, M., Kasten, M., Tunc, S., Sue, C. M., Svetel, M., Kostić, V. S., Segura-Aguilar, J., Ramirez, A. et al. (2012). Frequency of the D620N mutation in VPS35 in Parkinson disease. *Arch. Neurol.* **69**, 1360-1364.

Labrousse, A. M., Zappaterra, M. D., Rube, D. A. and van der Bliek, A. M. (1999). C. elegans dynamin-related protein DRP-1 controls severing of the mitochondrial outer membrane. *Mol. Cell* **4**, 815-826.

Lee, J. E., Westrate, L. M., Wu, H., Page, C. and Voeltz, G. K. (2016). Multiple dynamin family members collaborate to drive mitochondrial division. *Nature* **540**, 139-143.

MacLeod, D. A., Rhinn, H., Kuwahara, T., Zolin, A., Di Paolo, G., McCabe, B. D., Marder, K. S., Honig, L. S., Clark, L. N., Small, S. A. et al. (2013). RAB7L1 interacts with LRRK2 to modify intraneuronal protein sorting and Parkinson's disease risk. *Neuron* **77**, 425-439.

Melo, A. A., Hegde, B. G., Shah, C., Larsson, E., Isas, J. M., Kunz, S., Lundmark, R., Langen, R. and Daumke, O. (2017). Structural insights into the activation mechanism of dynamin-like EHD ATPases. *Proc. Natl. Acad. Sci. USA.* **114**, 5629-5634.

Nicholls, D. G. (2005). Mitochondria and calcium signaling. *Cell Calcium* **38**, 311-317.

Pitts, K. R., Yoon, Y., Krueger, E. W. and McNiven, M. A. (1999). The dynamin-like protein DLP1 is essential for normal distribution and morphology of the endoplasmic reticulum and mitochondria in mammalian cells. *Mol. Biol. Cell* **10**, 4403-4417.

Rojo, M., Legros, F., Chateau, D. and Lombes, A. (2002). Membrane topology and mitochondrial targeting of mitofusins, ubiquitous mammalian homologs of the transmembrane GTPase Fzo. *J. Cell Sci.* **115**, 1663-1674.

Santel, A. and Frank, S. (2008). Shaping mitochondria: The complex posttranslational regulation of the mitochondrial fission protein DRP1. *IUBMB Life* **60**, 448-455.

Santel, A. and Fuller, M. T. (2001). Control of mitochondrial morphology by a human mitofusin. *J. Cell Sci.* **114**, 867-874.

Sharma, M., Panapakkam Giridharan, S. S., Rahajeng, J., Naslavsky, N. and Caplan, S. (2009). MICAL-L1 links EHD1 to tubular recycling endosomes and regulates receptor recycling. *Mol. Biol. Cell* **20**, 5181-5194.

Sharma, M., Ioannidis, J. P. A., Aasly, J. O., Annesi, G., Brice, A., Bertram, L., Bozi, M., Barcikowska, M., Crosiers, D., Clarke, C. E. et al. (2012). A multi-centre clinico-genetic analysis of the VPS35 gene in Parkinson disease indicates reduced penetrance for disease-associated variants. *J. Med. Genet.* **49**, 721-726.

Struhal, W., Presslauer, S., Spielberger, S., Zimprich, A., Auff, E., Bruecke, T., Poewe, W, Ransmayr, G. and **The Austrian VPS-35 Investigators Team** (2014). VPS35 Parkinson's disease phenotype resembles the sporadic disease. *J. Neural Transm. (Vienna)* **121**, 755-759.

Taguchi, N., Ishihara, N., Jofuku, A., Oka, T. and Mihara, K. (2007). Mitotic phosphorylation of dynamin-related GTPase Drp1 participates in mitochondrial fission. *J. Biol. Chem.* **282**, 11521-11529.

Tang, F.-L., Liu, W., Hu, J.-X., Erion, J. R., Ye, J., Mei, L. and Xiong, W.-C. (2015). VPS35 deficiency or mutation causes dopaminergic neuronal loss by impairing mitochondrial fusion and function. *Cell Rep.* **12**, 1631-1643.

Vilariño-Güell, C., Wider, C., Ross, O. A., Dachsel, J. C., Kachergus, J. M., Lincoln, S. J., Soto-Ortolaza, A. I., Cobb, S. A., Wilhoite, G. J., Bacon, J. A. et al. (2011). VPS35 mutations in Parkinson disease. *Am. J. Hum. Genet.* **89**, 162-167.

Wang, C. and Youle, R. J. (2009). The role of mitochondria in apoptosis. *Annu. Rev. Genet.* **43**, 95-118.

Wang, C.-L., Tang, F.-L., Peng, Y., Shen, C.-Y., Mei, L. and Xiong, W.-C. (2012). VPS35 regulates developing mouse hippocampal neuronal morphogenesis by promoting retrograde trafficking of BACE1. *Biol. Open* **1**, 1248-1257.

Wang, W., Wang, X., Fujioka, H., Hoppel, C., Whone, A. L., Caldwell, M. A., Cullen, P. J., Liu, J. and Zhu, X. (2016). Parkinson's disease-associated mutant VPS35 causes mitochondrial dysfunction by recycling DLP1 complexes. *Nat. Med.* **22**, 54-63.

Wang, W., Ma, X., Zhou, L., Liu, J. and Zhu, X. (2017). A conserved retromer sorting motif is essential for mitochondrial DLP1 recycling by VPS35 in Parkinson's disease model. *Hum. Mol. Genet.* **26**, 781-789.

Yun, J., Puri, R., Yang, H., Lizzio, M. A., Wu, C., Sheng, Z. H. and Guo, M. (2014). MUL1 acts in parallel to the PINK1/parkin pathway in regulating mitofusin and compensates for loss of PINK1/parkin. *Elife* **3**, e01958.

Zhang, J., Reiling, C., Reinecke, J. B., Prislan, I., Marky, L. A., Sorgen, P. L., Naslavsky, N. and Caplan, S. (2012). Rabankyrin-5 interacts with EHD1 and Vps26 to regulate endocytic trafficking and retromer function. *Traffic* **13**, 745-757.

Zimprich, A., Benet-Pagès, A., Struhal, W., Graf, E., Eck, S. H., Offman, M. N., Haubenberger, D., Spielberger, S., Schulte, E. C., Lichtner, P. et al. (2011). A mutation in VPS35, encoding a subunit of the retromer complex, causes late-onset Parkinson disease. *Am. J. Hum. Genet.* **89**, 168-175.

Supplemental Information

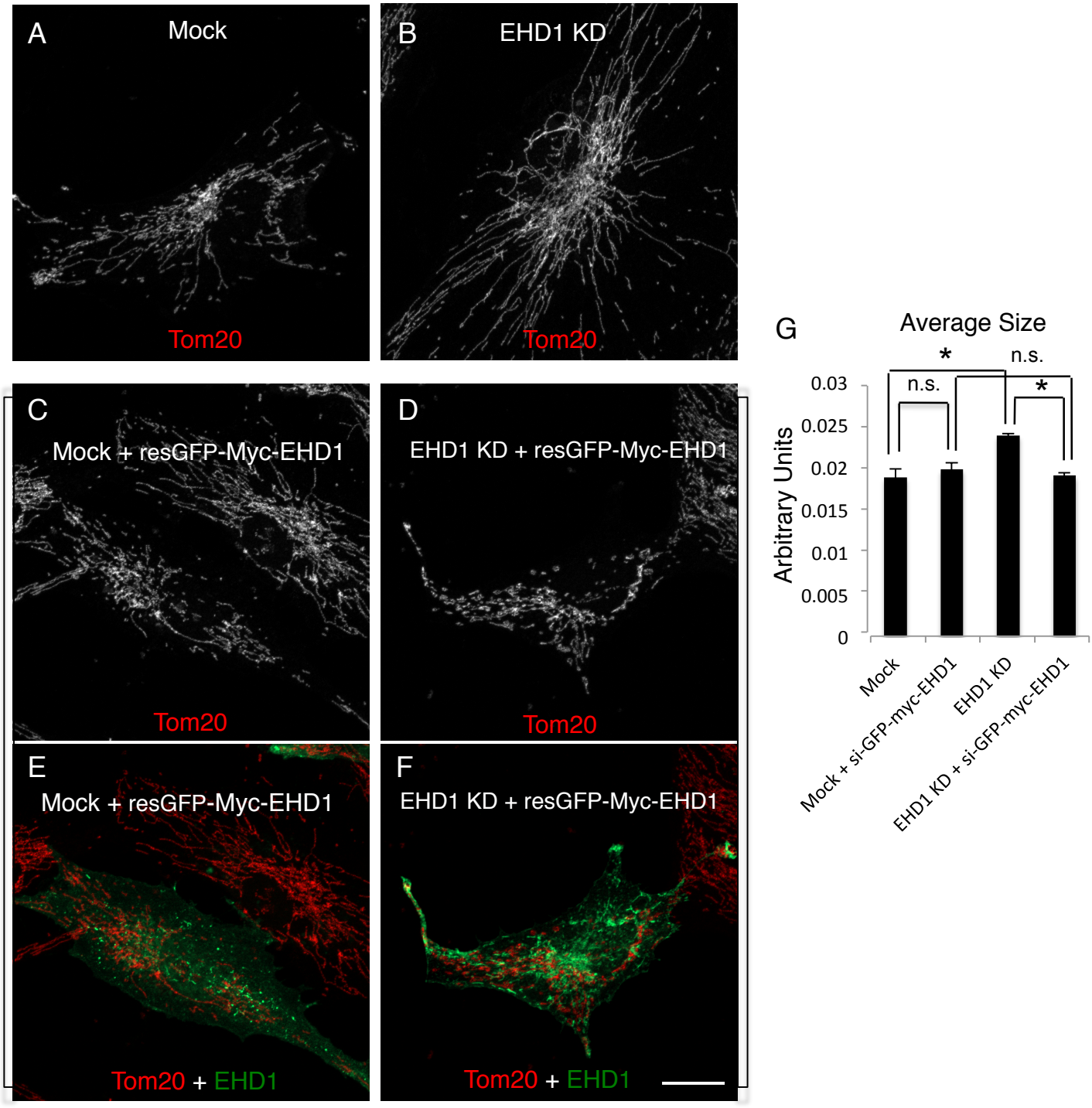

Supplemental Fig. 1. The elongated mitochondrial phenotype is rescued when EHD1 is reintroduced into EHD1 knock-down cells. (A-F) RPE cells were Mock-treated (A, C, E) or treated with EHD1-siRNA (B, D, F) for 72 h. Some of the cover-slips containing Mock or EHD1 knock-down cells were further transfected with an siRNA-resistant GFP-Myc-EHD1 cDNA (si-GFP-myc-EHD1) for the last 24 h (C-F). All cells were fixed and immunostained with antibodies against Tom20 (A-F). GFP-Myc-EHD1 transfected cells are seen in green, Bar, 10 μm. (G) At least 7 cells from each treatment (in 3 independent experiments) in A-F were analyzed by Mito Morphology Macro plugin in ImageJ and the mean+/-s.d. for size of their mitochondria was plotted. * denotes p values of less than 0.05, and n.s. denotes differences that are not statistically significant ($p>0.05$).

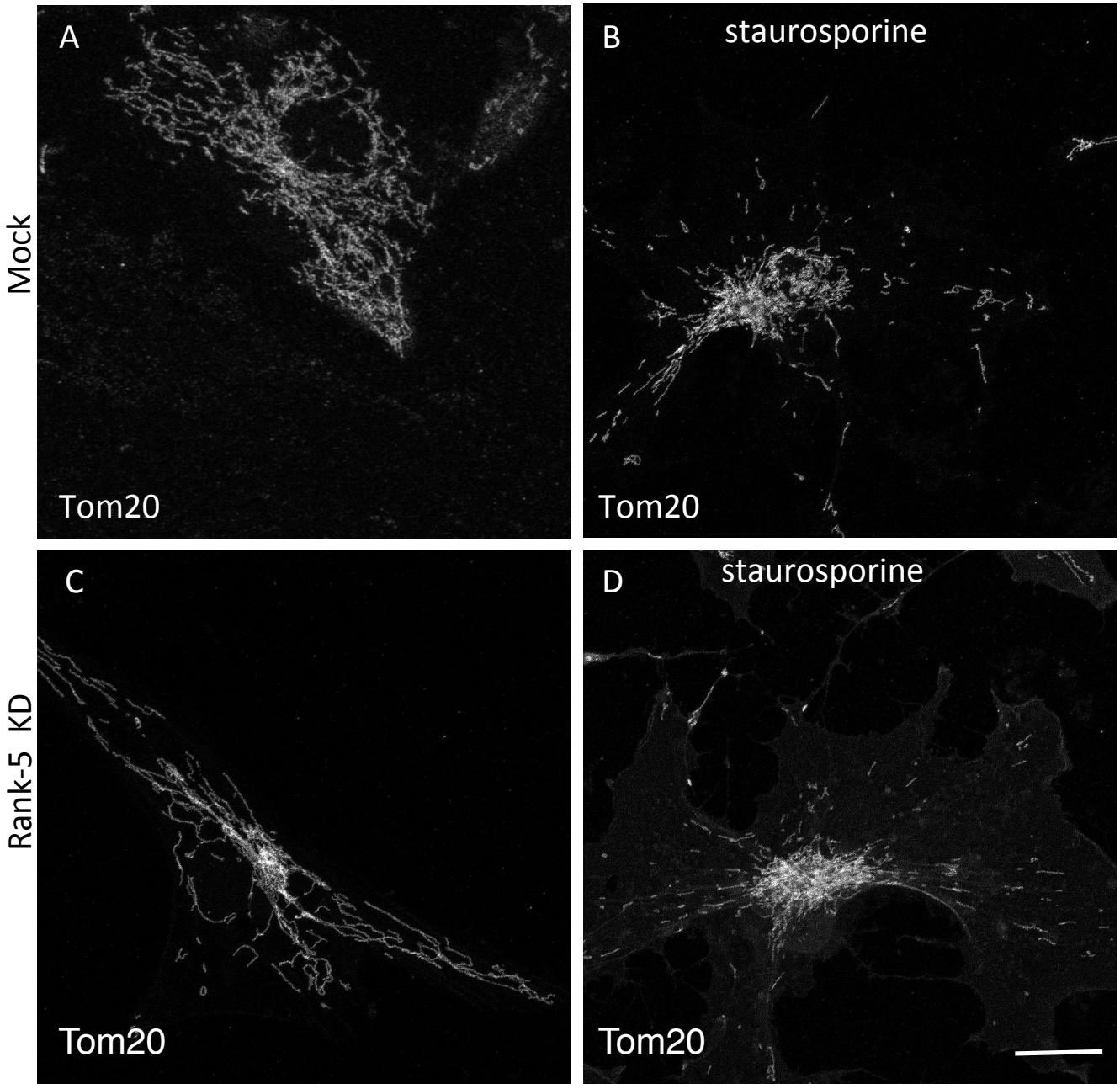

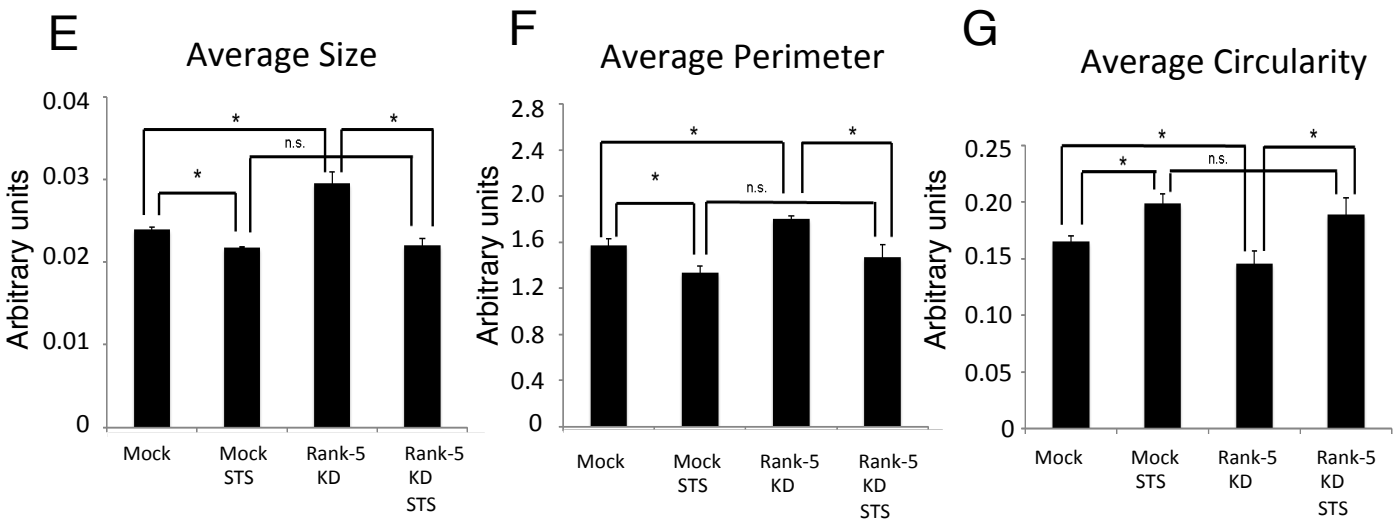

Supplemental Fig. 2. Rabankyrin-5 plays a regulatory role in mitochondrial fission. (A-D) RPE cells were either Mock-treated (A, B) or treated with Rabankyrin-5 siRNA for 72 h (C, D), followed by incubation with staurosporine for the last 1 h of treatment (B, D) or without the drug (A, C). (E-G) The Mito Morphology Macro plugin in ImageJ was used for quantifying average mitochondrial size, perimeter and circularity, and a one-tailed student's t-test was used to assess statistical significance. * denotes p values of less than 0.05, and n.s. denotes differences that are not statistically significant ($p>0.05$).

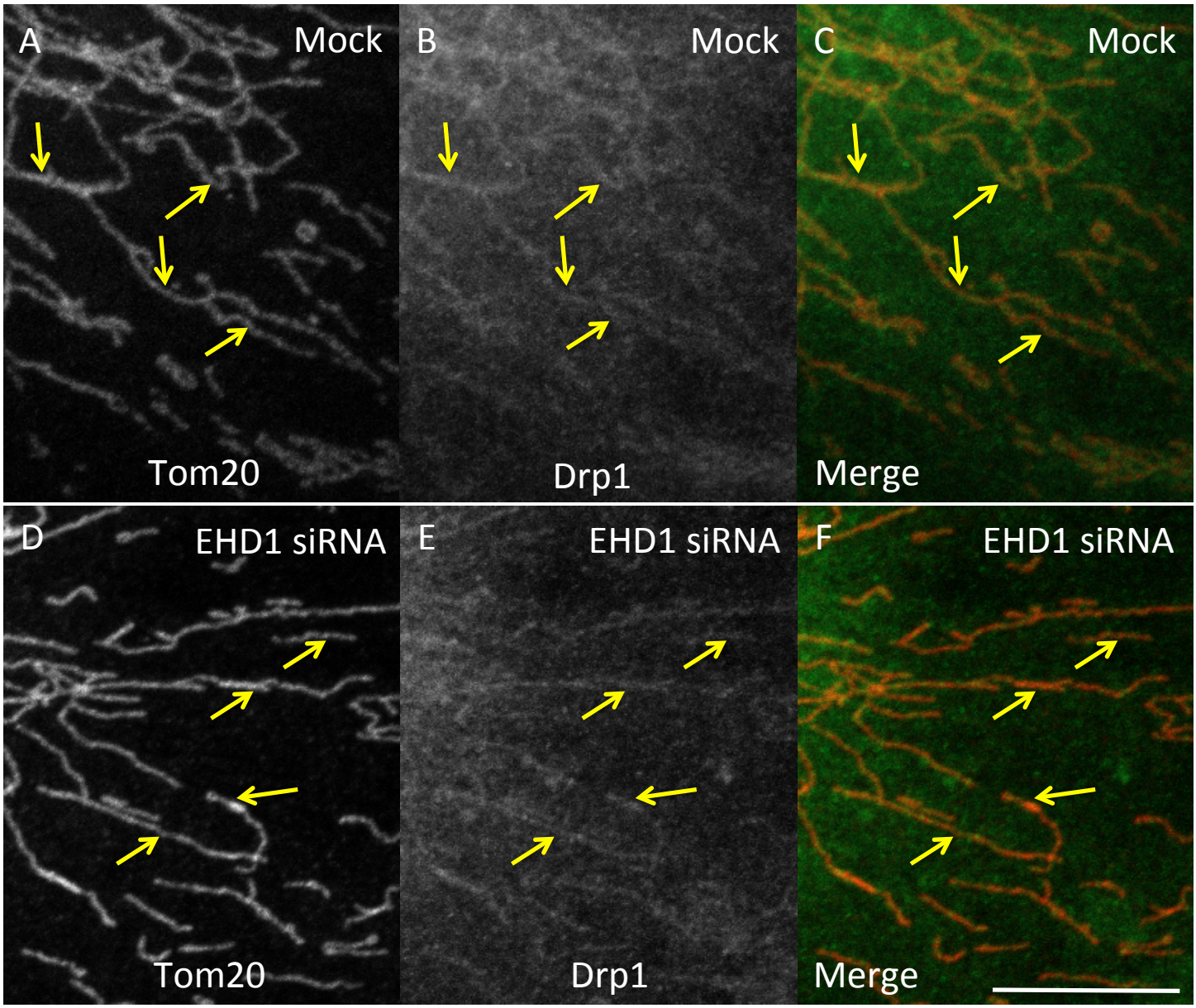

Supplemental Fig. 3. Drp1 localization to mitochondria is not significantly altered in the absence of EHD1. (A-F) RPE cells were either Mock-treated (A-C) or treated with EHD1-siRNA for 72 h (D-F), fixed, permabilized and immunostained with antibodies to Tom20 (A and D), and Drp1 (B and E). Merged images are depicted in C and F. Bar, 10 μm.

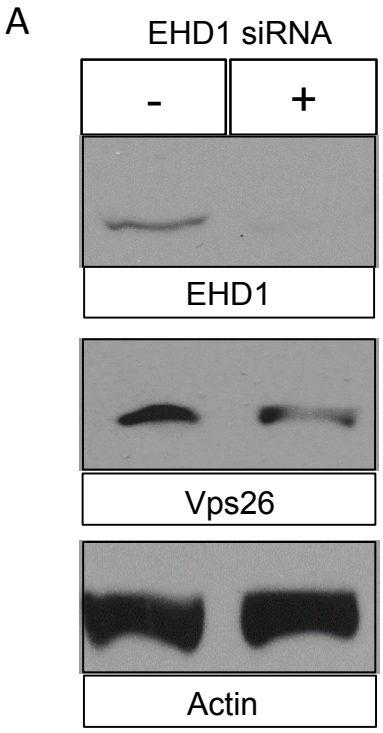

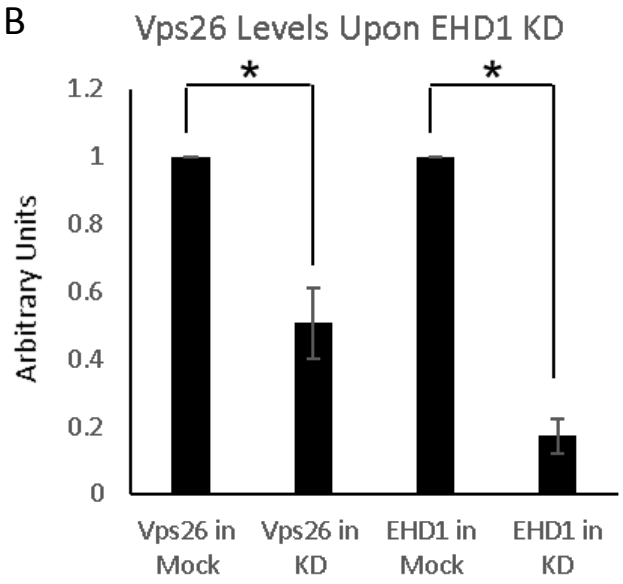

Supplemental Fig. 4. Depletion of EHD1 results in reduced VPS26. (A) HeLa cells were either Mock-treated, treated with EHD1- siRNA for 72 h and immunoblotted with VPS26, EHD1, and actin. (B) ImageJ was used to quantify the adjusted relative density of the immunoblot and a one-tailed student's t-test was used to assess statistical significance. * denotes p values of less than 0.05.

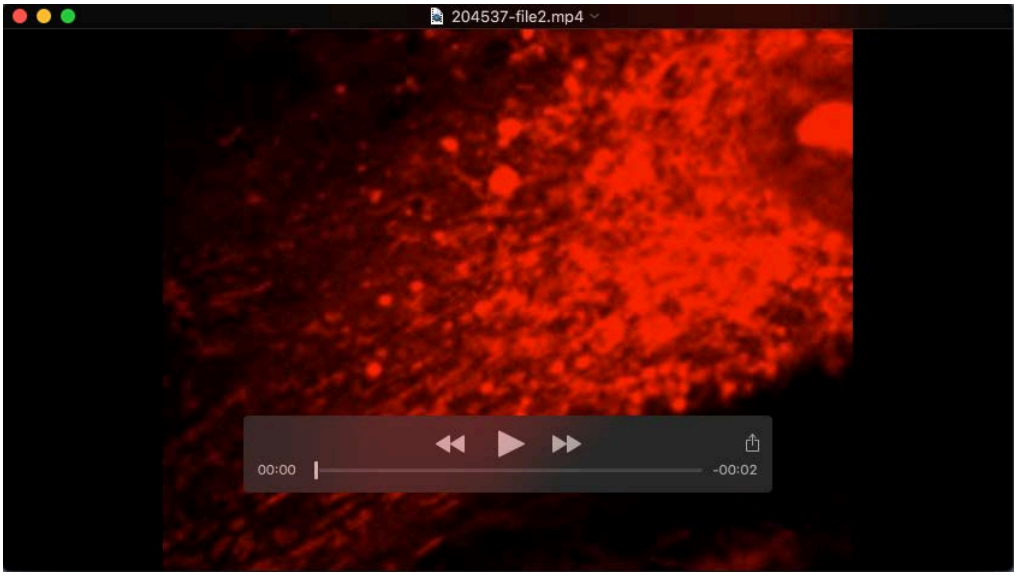

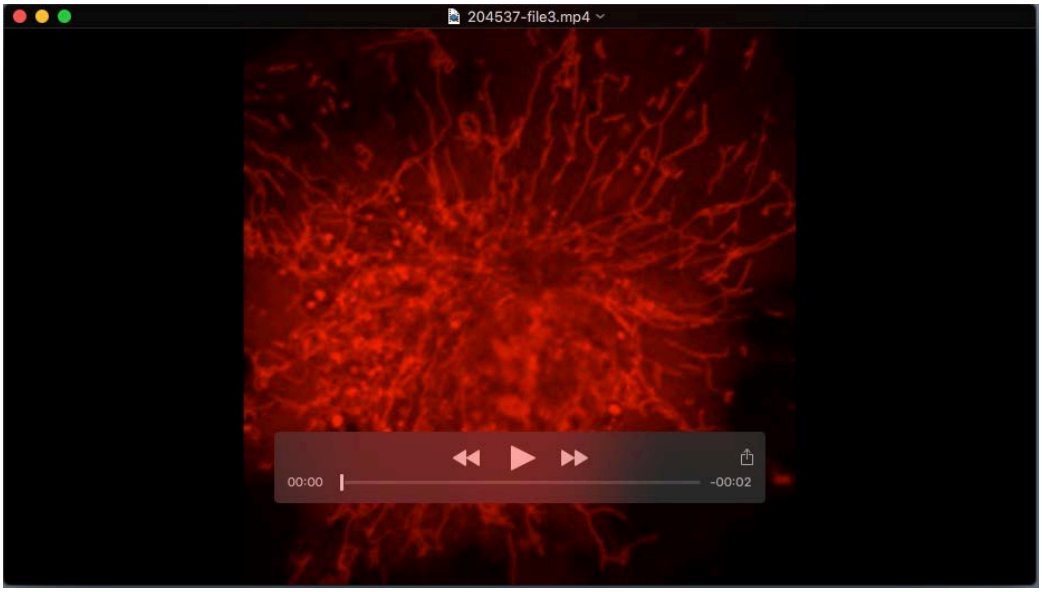

Journal of Cell Science • Supplementary information

Supplemental Movie 1 and Movie 2. Mitochondrial dynamics are impaired upon EHD1-depletion. Live imaging was performed on RPE cells incubated with Mitotracker Red and either Mock-treated (Supplemental Movie 1) or treated with EHD1-siRNA for 72 h (Supplemental Movie 2). 4-slice Z-section images were taken every 15 sec for 5 min for each treatment, and compiled to a maximal projection image.

Antibody Validation

Validation of the EHD1 and Rabankyrin-5 antibodies was done by siRNA knock-down showing the specific loss of the 60 kDa band in immunoblot (Fig. 1 and Fig. 5). The MICAL-L1 antibody was similarly validated in a previous study (Sharma et al., 2009). VPS26 and actin antibodies, as well as secondary antibodies coupled to fluorescent dyes or HRP were used by us previously (Zhang et al., 2012), and Tom20 antibodies have been previously used (Lee et al., 2016). The VPS35 antibodies have also been previously validated by knock-down and immunoblot (Zhou et al., 2016), as have the Mfn2 antibodies (Rakovic et al., 2011), the GM130 antibodies (Kodani and Sutterlin, 2008), and the Drp1 antibodies (Tang et al., 2016).